# Error Estimated Driven Anisotropic Mesh Refinement for Three-Dimensional Diffusion Simulation

Wilfried Wessner, Clemens Heitzinger, Andreas Hössinger, and Siegfried Selberherr
Institute for Microelectronics, TU Vienna, Gusshaustrasse 27-29, Vienna, Austria
Telephone: +43-1-58801/36031, Fax: +43-1-58801/36099, Email: Wessner@iue.tuwien.ac.at

*Abstract*— **We present a computational method for locally adapted conformal anisotropic tetrahedral mesh refinement. The element size is determined by an anisotropy function which is governed by an error estimation driven ruler according to an adjustable maximum error. Anisotropic structures are taken into account to reduce the amount of elements compared to strict isotropic refinement. The spatial resolution in three-dimensional unstructured tetrahedral meshes for diffusion simulation can be dynamically increased.**

## I. Introduction

In the numerical solution of practical problems of physics engineering such as semiconductor process and device simulation, one often encounters the difficulty that the overall accuracy of the numerical approximation is deteriorated by local exaltations. An obvious remedy is to refine the discretization in the critical regions [1]. The question then is how to identify these regions and how to obtain a good balance between the refined and unrefined regions such that the overall accuracy is optimal. These considerations clearly show the need for error estimators which can be extracted a posteriori from the computed numerical solution and the given data of the problem. The error should be local and should yield reliable upper and lower bounds. The global upper bounds are sufficient to obtain a numerical solution with an accuracy below a prescribed tolerance. Local lower bounds are necessary to ensure that the grid is correctly refined according to an adjustable error using a (nearly) minimal number of grid-points. As shown in Fig. 1, during the calculation of a time step a combination of error estimation and refinement mechanism is necessary to deliver higher accuracy, if needed, by increasing the spatial resolution.

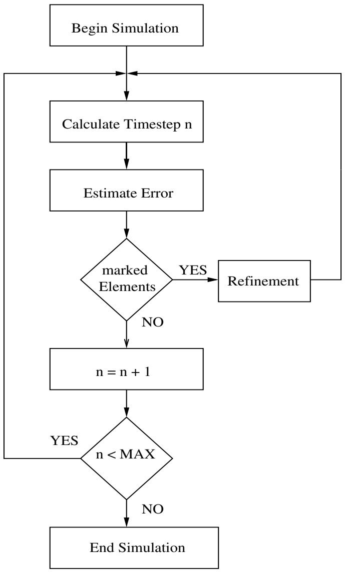

Fig. 1. Simulation procedure

## II. Anisotropic Refinement

Using strict isotropic meshes for three-dimensional process simulation is not practicable [2]. The need of calculation time and the limitation of memory tend to result in anisotropic adapted meshes which are more manageable. In [3], e.g., the element shapes are controlled by a tensor-based metric space for representing mesh anisotropy over the domain.

Anisotropy is defined by three orthogonal principal directions and an aspect ratio in each direction. The three principal directions are represented by three unit vectors $\vec{\xi}, \vec{\eta}$, and $\vec{\zeta}$, and in these directions the amounts of stretching of a mesh element are represented by three scalar values $\lambda_\xi, \lambda_\eta, \lambda_\zeta$, respectively. Using $(\vec{\xi}, \vec{\eta}, \vec{\zeta})$ and $(\lambda_\xi, \lambda_\eta, \lambda_\zeta)$ we define two matrices $\mathbf{R}$ and $\mathbf{S}$ by

$$\mathbf{R} := \begin{pmatrix} \xi_x & \eta_x & \zeta_x \\ \xi_y & \eta_y & \zeta_y \\ \xi_z & \eta_z & \zeta_z \end{pmatrix} \text{ and } \mathbf{S} := \begin{pmatrix} \lambda_\xi & 0 & 0 \\ 0 & \lambda_\eta & 0 \\ 0 & 0 & \lambda_\zeta \end{pmatrix}. \qquad (1)$$

By combining matrices $\mathbf{R}$ and $\mathbf{S}$, we obtain a $3 \times 3$ positive definite matrix $\mathbf{M}$

$$\mathbf{M} := \mathbf{R}\mathbf{S}\mathbf{R}^T \qquad (2)$$

that describes the three-dimensional anisotropy.

The basic refinement step in our algorithm is tetrahedral bisection which is well investigated by, e.g. Arnold [4]. When bisecting a tetrahedron, a particular edge – called the *refinement edge* – is selected and split into two edges by a new vertex. As new tetrahedra are constructed by refinement, their refinement edges must be selected carefully to take anisotropy into account without producing degenerately shaped elements. In order to identify which edge should be cut, the length of the edges is calculated in a metric space [5].

A set $S$ with a global distance function (the metric $g$) which for every two points $x, y$ in $S$ gives the distance between them as a nonnegative real number $g(x, y)$ is called the metric space [6].

0-7803-7826-1/03/$17.00 © 2003 IEEE

The distance function must also satisfy

$$\begin{aligned} &g(x,y)=0 \Leftrightarrow x=y \\ &g(x,y)=g(y,x) \\ &g(x,y)+g(y,z)\geq g(x,z). \end{aligned} \tag{3}$$

In our implementation this metric specially varies over the domain, and hence the length of an edge depends on its position. In case the *anisotropic length* is greater than an adjustable value, the edge is cut in the middle.

Calculating the length of an edge in a metric space can be seen as calculating a line integral. In general an arc length $\ell_C$ is defined as the length along a curve $C$: $\ell_C = \int_C ds$. $\mathbf{M}$ as defined in (2) represents a metric when viewed as positive definite tensor $\mathbf{M} = \mathbf{M}(x, y, z)$ over the entire domain. Roughly spoken, the metric tensor $\mathbf{m_{ij}}$ shows how to compute the distance between any two points in a given space. Its components can be viewed as multiplication factors which must be placed in front of the differential displacements $dx_i$ in a generalized Pythagorean theorem $ds^2 = g_{11}dx_1^2 + g_{12}dx_1dx_2 + g_{22}dx_2^2 + \cdots$.
The length of a line segment $PQ$ in a metric space is calculated by [7]

$$\ell_{PQ} = \int_0^1 \sqrt{PQ^T \cdot \mathbf{M}(P+tPQ)\cdot PQ}\, dt \tag{4}$$

where $\mathbf{M}(P+tPQ)$ is the metric at point $P+tPQ, t\in[0,1]$.

The basic idea of our refinement algorithm is to use the gradient field of the solution and the given data of the scalar diffusion problem as *stretching direction* of the anisotropy metric. The gradient $\nabla C = \text{grad}(C)$ of a scalar field $C = C(x, y, z)$ in Cartesian coordinates is given by

$$\nabla C = \frac{\partial C(x,y,z)}{\partial x}\vec{i} + \frac{\partial C(x,y,z)}{\partial y}\vec{j} + \frac{\partial C(x,y,z)}{\partial z}\vec{k}. \tag{5}$$

The gradient of a tetrahedral discretization can be calculated by using linear basis functions [8] applied to the three-dimensional unit simplex $T$. The coordinate transformation

$$\begin{aligned} x &= x_1 + (x_2-x_1)\zeta + (x_3-x_1)\eta + (x_4-x_1)\zeta \\ y &= y_1 + (y_2-y_1)\zeta + (y_3-y_1)\eta + (y_4-y_1)\zeta \\ z &= z_1 + (z_2-z_1)\zeta + (z_3-z_1)\eta + (z_4-z_1)\zeta \end{aligned} \tag{6}$$

allows to map an arbitrary tetrahedron at global coordinates $(x, y, z)$ to the unit simplex $T$ (cf. Fig. 2) with local element coordinates $(\xi, \eta, \zeta)$. In matrix notation this can be written as

$$\vec{r} - \vec{r_1} = \mathbf{J}\cdot\vec{\delta}, \tag{7}$$

where $\vec{r} = (x, y, z)^T$, $\vec{r_1} = (x_1, y_1, z_1)$, $\vec{\delta} = (\xi, \eta, \zeta)^T$, and $\mathbf{J}$ denotes the Jacobian

$$\mathbf{J} = \begin{pmatrix} x_2-x_1 & x_3-x_1 & x_4-x_1 \\ y_2-y_1 & y_3-y_1 & y_4-y_1 \\ z_2-z_1 & z_3-z_1 & z_4-z_1 \end{pmatrix}. \tag{8}$$

Using linear basis functions on the three-dimensional unit simplex, which are given by [9]

$$\begin{aligned} N_1 &= 1-\xi-\eta-\zeta \\ N_2 &= \xi \\ N_3 &= \eta \\ N_4 &= \zeta, \end{aligned} \tag{9}$$

allows a linear approximation over the element in the form

$$C(\xi,\eta,\zeta) = \sum_{k=1}^{4} N_k(\xi,\eta,\zeta)C_k, \tag{10}$$

where $C_k$ denotes the scalar value of the solution on vertex $k$ of the three-dimensional unit simplex $T$.

Applying (5) to the linear approximation, given by (10), results in

$$\nabla C(\xi,\eta,\zeta) = \begin{pmatrix} -C_1+C_2 \\ -C_1+C_3 \\ -C_1+C_4 \end{pmatrix} \tag{11}$$

for the gradient of the discretization. The gradient is constant over an element and represents the anisotropic stretching direction.

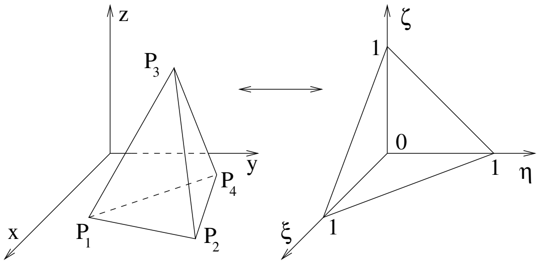

Fig. 2. Coordinates transformation.

## III. Diffusion

Diffusion is the transport of matter caused by a gradient of the chemical potential. This mechanism is responsible for the redistribution of dopant atoms within a semiconductor during a high-temperature processing step. The underlying ideas can be categorized into two major approaches, namely, the continuum theory of Fick's diffusion equation and the atomistic theory [10]. We are using the continuum theory approach which describes the diffusion phenomenon by the diffusion law:

$$\vec{J} = -D\cdot\text{grad}(C) \tag{12}$$

$\vec{J}$ denotes the diffusion flux, $D$ is the *diffusion coefficient* or *diffusivity*, and $C$ is the concentration of the dopant atoms.
In general, the diffusion models used in semiconductor process simulation are strongly nonlinear, because the diffusion coefficients depend, e.g., on the impurity and point defects [11]. These dependences also couple the equations for multiple impurities and point defects. Additionally, more

complex models include chemical reactions and contain convection terms. However, for better understanding of our refinement method we use the linear parabolic diffusion problem which is given by (12).

## IV. Error Estimation

Since the vector field $\nabla C(\xi, \eta, \zeta)$ (11) is piecewise constant, it is obvious that strong variations of the gradient from one element to an adjacent one yield an approximation error when compared to the proper continuous gradient field. This gradient approximation error causes a diffusion flux error which gives rise to a violation of the law of mass conservation.

According to the discussion of a posteriori gradient recovery error estimation by Ainsworth [12], the basic idea is to estimate the error per cell by integrating the gradient jump of the solution along the faces of each cell.

For the elliptic problem $-\nabla(a(x)\triangle u) = f$ with Dirichlet boundary conditions, an error estimator for two dimensional triangulations, proposed by Kelly et al. [13], is

$$\eta_K^2 = \frac{h}{24}\int_{\partial K} \left[\tfrac{\partial u_h}{\partial n}\right]^2 d\sigma, \tag{13}$$

where $h$ denotes the longest edge of the triangle $K$ and $\left[\omega\right]_K(x) := \lim_{\epsilon\to 0+}\omega(x+\epsilon\nu_K) - \lim_{\epsilon\to 0+}\omega(x-\epsilon\nu_K), x \in K$, is the jump of $\omega$ over the triangle $K$.

Picking up this idea for elliptic problems we use a modification for the linear parabolic diffusion problem (12). In our implementation the error estimation is performed by calculating the gradient field of the solution in every element over the domain, where only a small variation in adjacent vectors is allowed. As shown in Fig. 3, to evaluate the variation, the maximum of the vector norm of the difference

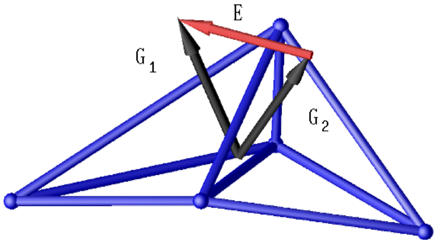

Fig. 3. Error of adjacent gradient vectors.

$$\ell_d = \|\vec{E}\|_2 = \sqrt{(\vec{G_1}-\vec{G_2})\cdot(\vec{G_1}-\vec{G_2})} \tag{14}$$

of adjacent gradient vectors $G_1$ and $G_2$ is used. For this procedure only the face-to-face relationship of every tetrahedron is used. So in this sense every tetrahedron has as maximum only four neighbors. The length of the difference vector $\ell_d$ can be seen as measure for the anisotropic *stretching values* (1). The refinement anisotropy is now fully described by the stretching direction (the gradient field) and the stretching values (length of the difference vectors).

According to Section I an adjustable lower bound for the whole discretized domain is necessary to identify which regions should be refined. As shown in Fig. 1 after error estimation critical elements are marked for the refinement procedure if $\ell_d$ (14) is greater than the prescribed lower error bound. The refinement procedure utilizes the local element gradient as anisotropy direction in combination with (14) to identify which edge of the marked tetrahedron should be used for the new vertex.

## V. Example

To see the essential impact of our refinement strategy we use a three-dimensional test structure. The underlying initial mesh (see Fig. 4) is a coarse fairly isotropic mesh which carries a dopant profile. The white area can be seen as mask, where at the upturn open part of the structure the diffusion dose $N_d$ is kept constant. For an one-dimensional case this can be written as

$$N_d = \int_0^\infty C(x,t)dx = \text{const.} \tag{15}$$

This diffusion condition is referred to as *drive-in diffusion* [14]. Note that the gradient of the concentration $C$ vanishes at the surface, $\nabla C = \text{grad}(C) = 0$, and so does the diffusion flux $\vec{J}$ (12). The dopant concentration has its maximum therfore at the step of the structure.

Fig. 5 shows the corresponding gradient field and iso-surfaces of the dopant concentration. The gradient vectors are calculated over every tetrahedron according to (11). The orientation of the gradient is turned towards higher concentration values and perpendicular to the iso-surfaces of the dopant concentration. The gradient field varies much stronger along the short edges of the structure.

To increase the accuracy, refinement is needed only in the relevant area around the step in the structure. The anisotropy should care of the variations of the vector field along the short edge of the structure and should keep the edge length along the long side.

As shown in Fig. 6, after refinement the edge length along the long side of the cuboid does not change much, but on the short side a much higher mesh density arises and the resolution can be increased. To find a good balance between refined and unrefined regions under consideration of element shapes its mandatory also to refine elements which belong to the white mask structure. Bisecting a tetrahedron by inserting a new vertex on an edge yields always the division of the whole patch. Well behaved element shapes demand a smooth transition between refined and unrefined regions. The algorithm produces a quite local refinement under consideration of a desired anisotropic behavior.

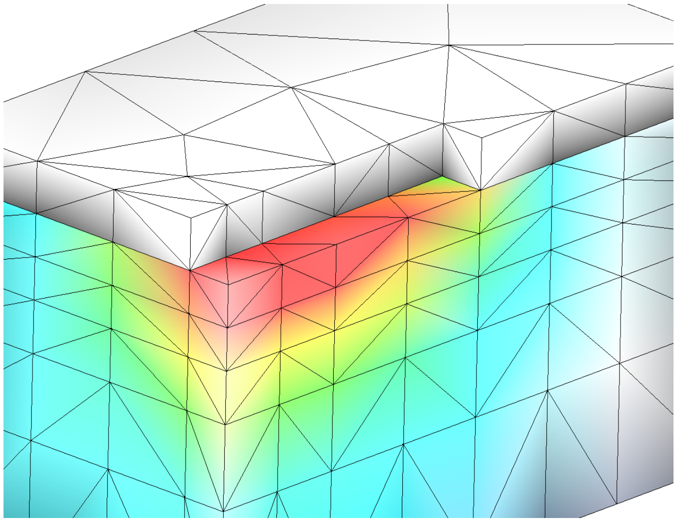

Fig. 4. Dopant concentration (initial mesh).

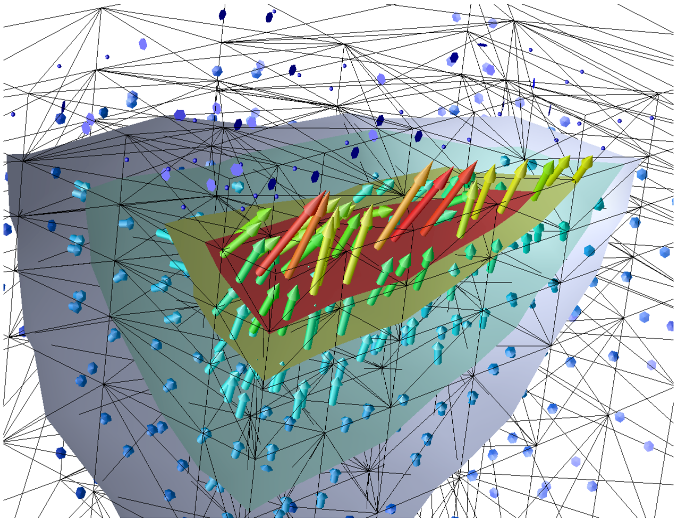

Fig. 5. Gradient field and iso-surfaces (initial mesh).

## VI. Conclusion

We present a computational method for anisotropic mesh refinement. The refinement method is based on bisecting tetrahedrons by inserting a new vertex on a particular edge. This particular edge is selected according to a specific metric which is governed by the gradient field of the numerical solution of the linear diffusion problem and the given initial data. The refinement is driven by an a posteriori error estimator which identifies these regions where a higher spatial resolution is needed. The algorithm shows a local behavior and avoids ill shaped elements during refinement. The resulting mesh matches the dopant profile appropriately and a good resolution of the gradient field is expected. Therefore this refinement method is also a good choice for complex dynamic diffusion problems.

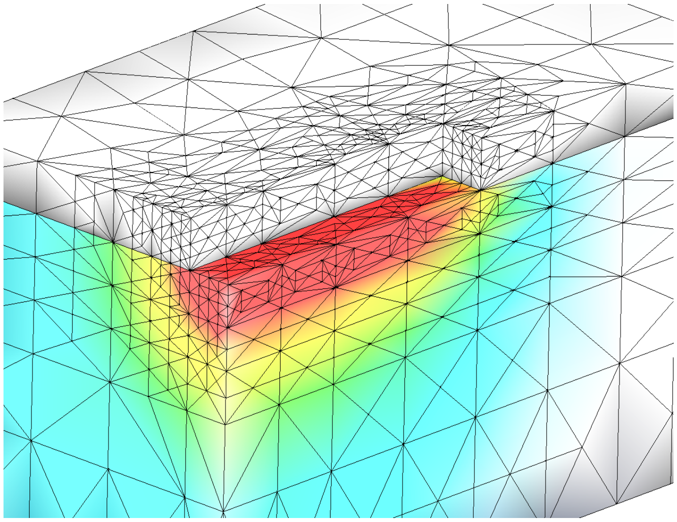

Fig. 6. Refined anisotropic mesh.

## References

[1] R. Verfürth, *A Review of A Posteriori Error Estimation and Adaptive Mesh-Refinemnet Techniques*, 1st ed. Baffins Lane, Chichester, West Sussex PO19 IUD, England: John Wiley & Sons Ltd. and B. G. Teubner, 1996.

[2] P. J. Frey and P.-L. George, *Mesh Generation*, 1st ed. 9 Park End Street, Oxford, OX1 1HH, United Kingdom: HERMES Science Europe Ltd, 2000.

[3] S. Yamakawa and K. Shimada, "High quality anisotropic tetrahedral mesh generation via ellipsoidal bubble packing," *Proceedings of 9th IMR*, pp. 263–273, 2000.

[4] D. N. Arnold, A. Mukherjee, and L. Pouly, "Locally adapted tetrahedral meshes using bisection," *SIAM J. Sci. Comput.*, vol. 22, no. 2, pp. 431–448, 2000.

[5] S. Lo, "3D anisotropic mesh refinement in compliance with a general metric specification," *ELSEVIER Finite Elements in Analysis and Design*, vol. 38, pp. 3–19, 2001.

[6] L. Kelly, *The geometry of metric and linear spaces*. Tiergartenstr. 17, D-69121 Heidelberg, Germany: Springer, 1975.

[7] H. Borouchaki, P. L. George, F. Hecht, P. Laug, and E. Saltel, "Delaunay mesh generation governed by metric specifiactions. Part I. Algorithms," *ELSEVIER Finite Elements in Analysis and Design*, vol. 25, pp. 61–83, 1997.

[8] O. Zienkiewicz and R. Taylor, *The Finite Element Method*, 4th ed. Shoppenhangers Road, Maidenhead, Berkshire, England: McGRAW-HILL Book Company Europe, 1989, vol. 1.

[9] R. Bauer, "Numerische Berechnung von Kapazitäten in dreidimensionalen Verdrahtungsstrukturen," Dissertation, Institut für Mikroelektronik, Technische Universität Wien, November 1994, `http://www.iue.tuwien.ac.at/`.

[10] Y. Nishi and R. Doering, *Handbook of Semiconductor Manufacturing Technology*, 1st ed. 270 Madison Avenue, New York, NY 10016: Marcel Dekkar, Inc., 2000.

[11] R. Kosik, P. Fleischmann, B. Haindl, P. Pietra, and S. Selberherr, "On the interplay between meshing and discretization in three-dimensional diffusion simulation," *IEEE Trans. Computer-Aided Design*, vol. 19, no. 11, pp. 1233–1240, November 2000.

[12] M. Ainsworth and J. T. Oden, "A posteriori error estimation in finite element analysis," *ELSEVIER Comput. Methods Appl. Mech. Engrg.*, vol. 142, pp. 1–88, 1997.

[13] D. W. Kelly, J. R. Gago, O. C. Zienkiewicz, and I. Babuska, "A posteriori error analysis and adaptive processes in the finite element method. Part I - Error analysis," *Int. J. Numer. Methods Engrg.*, vol. 19, pp. 1593–1619, 1983.

[14] P. Shewmon, *Diffusion in Solids*, 2nd ed. 420 Commonwealth Drive, Warrendale, Pennsylvania 15086, USA: Minerals, Metals & Materials Society, 1989.